

Development of a Momentum Determined Electron Beam in the 1 - 45 GeV Range

V.A. Batarin^d, J. Butler^a, A.A. Derevschikov^d, Yu.V. Fomin^d,
V. Frolov^b, V.N. Grishin^d, V.A. Kachanov^d, V.Y. Khodyrev^d,
A.S. Konstantinov^d, V.I. Kravtsov^d, Y. Kubota^b,
V.M. Leontiev^d, V.A. Maishev^d, Ya.A. Matulenko^d,
A.P. Meschanin^d, Y.M. Melnick^d, N.G. Minaev^d,
V.V. Mochalov^d, D.A. Morozov^d, L.V. Nogach^d,
P.A. Semenov^{d,1}, K.E. Shestermanov^d, L.F. Soloviev^d,
V.L. Solovianov^{d,2}, S. Stone^c, M.N. Ukhanov^d,
A.V. Uzunian^d, A.N. Vasiliev^d, A.E. Yakutin^d J. Yarba^a,

BTeV electromagnetic calorimeter group

^a*Fermilab, Batavia, IL 60510, U.S.A.*

^b*University of Minnesota, Minneapolis, MN 55455, U.S.A.*

^c*Syracuse University, Syracuse, NY 13244-1130, U.S.A.*

^d*Institute for High Energy Physics, Protvino, Russia*

Abstract

A beam line for electrons with energies in the range of 1 to 45 GeV, low contamination of hadrons and muons and high intensity up to 10^6 per accelerator spill at 27 GeV was setup at U70 accelerator in Protvino, Russia. A beam tagging system based on drift chambers with 160 μm resolution was able to measure relative electron beam momentum precisely. The resolution σ_p/p was 0.13% at 45 GeV where multiple scattering is negligible. This test beam setup provided a possibility to study properties of lead tungstate crystals (PbWO_4) for the BTeV experiment at Fermilab.

¹ corresponding author, email: semenov@mx.ihep.su

² deceased

1 Introduction

BTeV is a new experiment being prepared at FNAL, USA [1]. It is aimed at challenging the Standard Model explanation of CP-violation, mixing and rare decays in the b - and c -quark systems. To study final states containing photons, an electromagnetic calorimeter using lead tungstate (PbWO_4) scintillating crystals will be used. The energy resolution of this type of calorimeter is expected to be better than 1% for photon (or electron) energies above 10 GeV. We need to measure the resolution with a beam able to span a wide range of electron energies and yet having a low contamination of hadrons and muons. The energy of each beam electron should be known with a precision significantly less than 1%. An electron beam in the energy range of 1 to 45 GeV which satisfies the above requirements has been commissioned at the U70 accelerator at Protvino, Russia.

We determine the energy of each individual electron using a beam tagging system, since the natural energy spread of the beam is $\approx 3\%$ at 27 GeV. The tagging system consists of a spectrometer magnet and four drift chamber stations. In order to decrease multiple scattering, the beam was transported in vacuum. This system was able to measure the beam particle momentum with a precision of 0.13% at 45 GeV, where the contribution of multiple scattering is negligible. At 1 GeV a precision of momentum measurements was 2%, where multiple scattering dominated.

It is worth noting that, we measure the absolute value of the beam momentum to 1-2% accuracy, not as well as the above resolution. It is due to the accuracy of the spectrometer magnetic field measurements. For our studies of the electromagnetic calorimeter prototype we do not need to know the absolute value of the beam energy with a very high precision since the energy resolution does not strongly depend on energy.

The high intensity of the electron beam (up to 1×10^6 per accelerator spill at 27 GeV) and low background provide a good environment to study crystal radiation hardness. The same beam channel was able to provide a high intensity (up to 10^7 per accelerator spill) 40 GeV pion beam.

2 General beam setup

A method to obtain an electron beam from U70 proton beam is based on decays of neutral mesons (mainly π^0 -mesons) from the proton beam interactions on an internal carbon film target [2]. Photons from π^0 -decays are converted to electrons in an additional target (Converter1) made of ≈ 3 mm ($0.7X_0$)

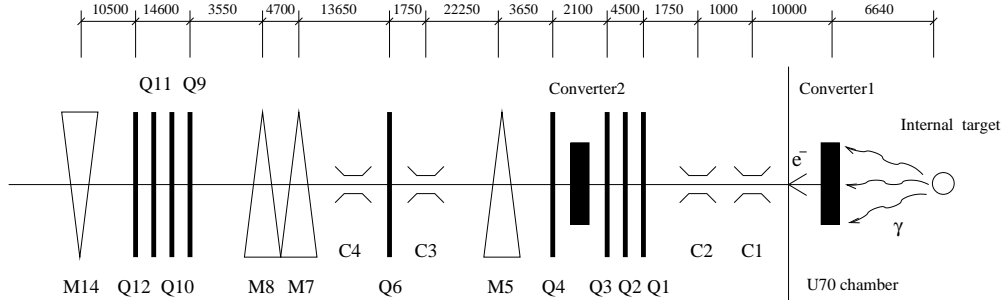


Fig. 1. Beam optics diagram. Q - quadrupole lenses, M - dipole magnets, C - collimators. Distances are in mm.

thickness Pb plate placed 6.6 m from the internal target. (see Fig.1). Charged hadrons from the internal target are swept away from the γ -quanta path by the U70 accelerator magnetic field and don't enter the beam line. A small number of hadrons in the electron beam are produced by neutron interactions with Converter1. Electrons from Converter1 are guided by the accelerator magnetic field to the beam line entrance. The output electron beam momentum is defined by the radial position of the internal target. The Converter1 placement in the accelerator chamber allows to obtain more intense beams (10^6 electrons per 10^{12} protons) but reduces the available electron beam momentum range to 25-45 GeV.

A further decreasing of initial momenta of electrons was obtained using an oriented silicon crystal [4] (Converter2) which was placed before the analyzing magnet M5. The electron beam after Converter2 has a wide momentum spectrum due to Bremsstrahlung radiation. The fields of the magnetic elements are setup proportionally to a beam momentum. Finally we have electron beam with any required energy from 1 GeV up to 45 GeV. It usually took us about 15 minutes to tune the beam line elements for given energy.

3 Beam tagging system

The beam momentum spread was $\Delta p/p \approx 3\%$ at 27 GeV and was too large to study the energy resolution of PbWO_4 crystals. So we decided to install momentum tagging system to measure the momentum of each electron. It consisted of four drift chamber stations (DC) and a 4 meter long spectrometer magnet denoted M14 (see Fig. 2). The magnet deflected the beam in the horizontal plane by 55 mrad. The magnet current was adjustable in order to provide the same bending angle for all energies of the electron beam.

The X and Y positions of the charged particle were measured in each DC station with a pair of drift chambers in each view, which shared the same gas volume. Each chamber has a 20×20 cm² sensitive area. The third station,

DC3, has only a pair of chambers measuring the x coordinate. All together four DC stations consisted of fourteen drift chambers.

The internal structure of a pair of drift chambers is shown in Fig. 3. Each drift cell is formed by a signal (sense) wire in the center, field wires at the edges of the cell and cathode planes perpendicular to the beam direction. The signal wires are separated by 2.4 cm corresponding to a maximum drift distance of 1.2 cm. The signal wires of the second chamber were shifted by 1.2 cm to resolve the left-right ambiguity. The distance between signal wires and cathode planes is 5 mm. The signal wires were made of gold plated tungsten ($20 \mu\text{m}$ diameter) and field wires, beryllium-copper alloy ($100 \mu\text{m}$ diameter). The cathode planes were made of graphite coated ($5 \mu\text{m}$) mylar (total thickness $25 \mu\text{m}$). To complete the electrostatic shielding of the modules, aluminized mylar ($25 \mu\text{m}$ mylar and less than $1 \mu\text{m}$ Al) was placed on the sides of the box.

Each chamber required two high voltages: the cathode voltage (HVC), and the voltage on the field wires (HVF) to make a uniform electric field along the cell. During the experiment all chambers were operated with HVC= -1.8 kV and HVF= -2.9 kV.

A mixture of argon (70%) and isobutane (30%) gas was used. The operating voltages gave a field gradient of 1 kV/cm in the main part of the drift space,

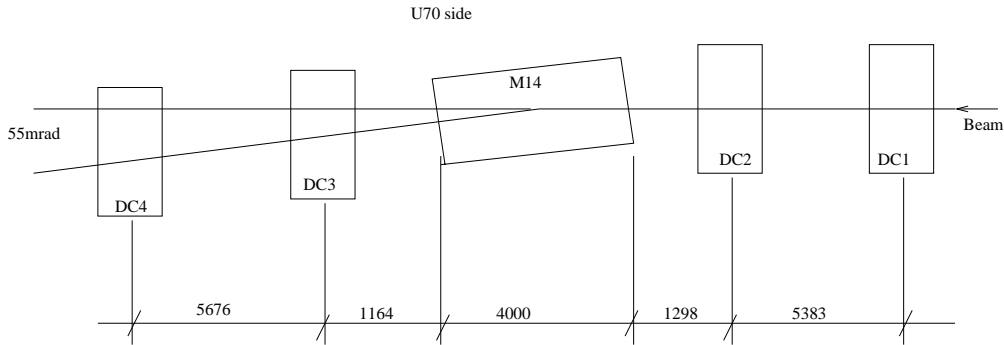


Fig. 2. The beam momentum tagging system. DC indicates a set of drift chambers, while M14 is a dipole bending magnet. (All distances are in mm.)

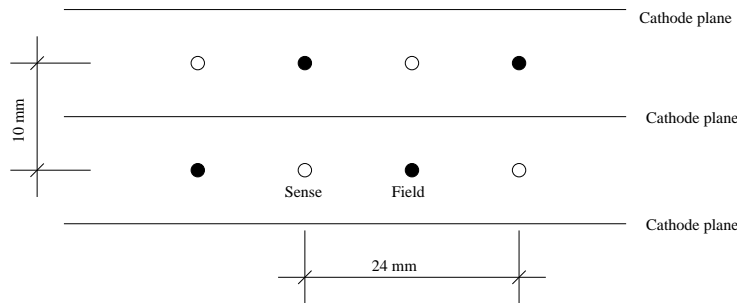


Fig. 3. The structure of each drift chamber doublet for a single view.

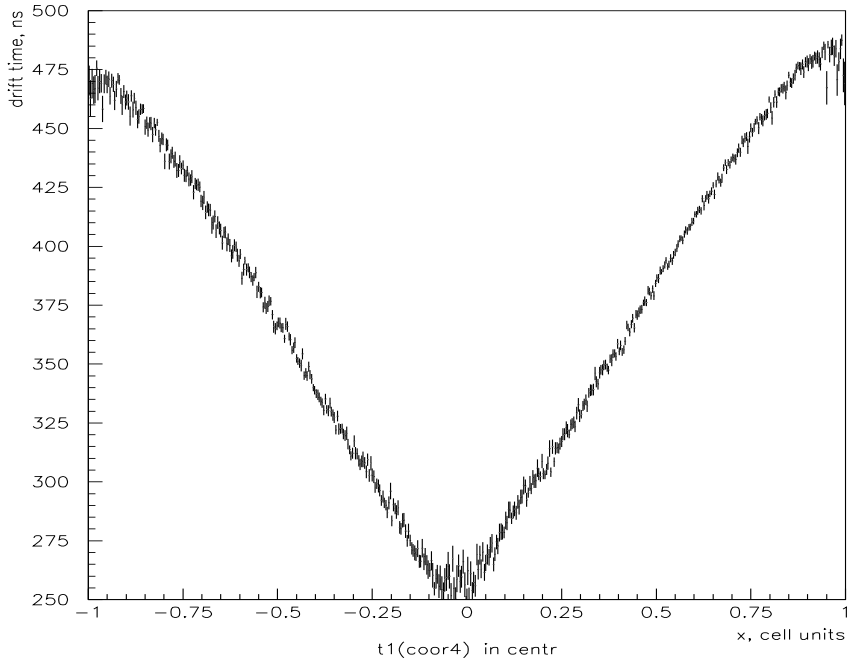


Fig. 4. Drift time versus track position dependence.

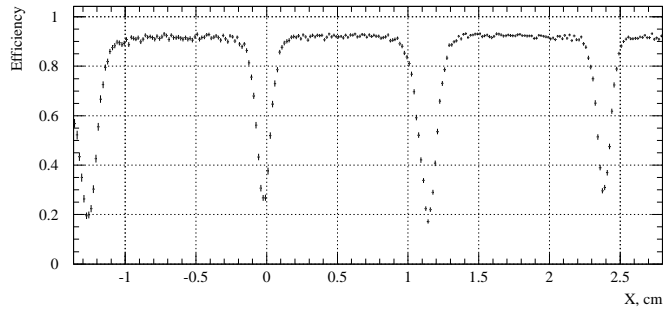


Fig. 5. A cell efficiency for the x-plane of the drift chamber DC2. $X=0$ corresponds to the sense wire position in the first subplane. Minima are caused by and correspond to the field wire positions both in the first and shifted subplanes.

which is enough to provide for a saturated drift velocity.

The design of the DC internal structure and operating voltages were the result of a compromise between predictions of a GARFIELD simulation for a constant drift velocity within the drift cell, track detection efficiency, and our requirement of minimum materials.

Assuming that the drift velocity is constant over the entire cell, we achieved the required track precision. The actual measured time distribution function for one of the drift chambers, $t(x)$, is shown in Fig. 4 where x was obtained from

a track fit over the three other DC stations. It shows some non-uniformity, so the precision of the track reconstruction can be improved further by fitting the drift velocity as a function of x . The DC efficiency is shown in Fig. 5. We reach the $\sim 90\%$ level over most of the cell. The drift time was measured by LeCroy 3377 TDC with a 1 ns/count accuracy.

4 Contamination of hadrons and muons in the electron beam

The fraction of electrons in the beam for various momenta were estimated in the following way. At the end of the beam line, after DC4 (see Fig.2), we place a box containing a 5×5 matrix of lead tungstate scintillating crystals. Using information from the drift chambers, beam particles which hit within a 3×3 region in the center of the crystal matrix have been selected. The crystals are square, 27 mm on each of the lateral side and 220 mm in length. For these events, the energy deposit in the entire calorimeter was measured.

Fig 6 shows the distribution of these measured energies for 10 GeV electron beam data. This is the worst case in terms of electron beam purity. We see clean muon and electron peaks at about ≈ 0.3 GeV and ≈ 10 GeV, respectively and the energy deposit from hadronic showers between them. The relatively large muon fraction was useful to monitor the stability of the calorimeter prototype properties.

The events with the energy deposit greater than 0.9 of MEAN value of the peak corresponding to the beam energy have been assigned to electrons. The rest of the events are background particles, muons and hadrons. The measured fractions of electrons in the beam for each beam energy are shown in Table 1. All fractions are determined to an absolute accuracy of 1%.

Table 1
Fraction of electrons in the beam at various energies

1 GeV	2 GeV	5 GeV	10 GeV	27 GeV	45 GeV
82%	77%	50%	34%	77%	91%

Note that by selecting events using drift chamber information, we rejected all charged particles which have momenta outside of the tagging station fiducial region. So, the obtained result does not reflect the total contamination of the hadrons and muons in the electron beam, which is estimated to be 25% more for 27 GeV.

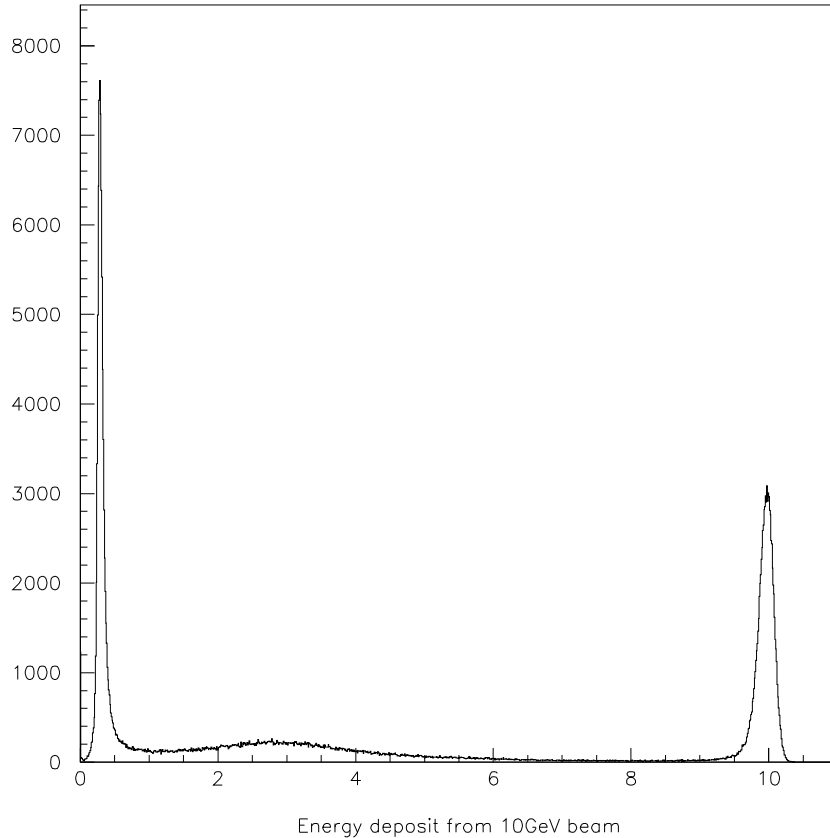


Fig. 6. Energy spectrum of the 10 GeV electron beam. This is the worst case in terms of a purity of the obtained electron beam.

5 Precision of the beam momentum measurement

In this section we estimate the accuracy of the beam momentum determination with our spectrometer. The design of the spectrometer was optimized for precision charged-particle tracking and momentum determination, as well as for precise position measurements of high energy electrons in the lead tungstate 5×5 electromagnetic calorimeter prototype.

The momentum resolution σ_p/p of the spectrometer equals the accuracy σ_θ/θ , where θ is the deflection angle in the analyzing a magnet. This angle is calculated from the linear combination of the 4 position measurements:

$$\theta \approx \sum_{i=1}^4 b_i \cdot x_i + c_{survey} \quad (1)$$

where b_i are the coefficients which depend on the distance of the chambers

from the analyzing magnet center, x_i 's are transverse coordinates of the beam particle measured in the drift chambers, and c_{survey} is a survey constant.

Two factors contribute to σ_θ , the uncertainty in the θ measurements. The first one is a drift chamber resolution. The second is a multiple Coulomb scattering on materials in the beam line. The main contribution of Coulomb scattering to the σ_θ is given by materials of the DC2 and DC3 stations since they are near the magnet (see Fig.2).

If we assume that all the drift chambers have the same position resolution σ_x , then

$$\sigma_\theta^2 = \sigma_x^2 \cdot \sum_{i=1}^4 b_i^2 + \sigma_{\theta_{Coulomb}}^2 \quad (2)$$

To define σ_θ^2 at different energies one needs to know the drift chamber position resolution and the mean multiple scattering angle. These values can be determined experimentally. We extrapolated the beam trajectories reconstructed by the upstream drift chambers (DC1 and DC2) and downstream drift chambers (DC3 and DC4) to the center of the analyzing magnet. Their lateral position (distance to the nominal beam position) should agree. We defined their difference as D_x , which can be calculated from another linear combination of the four x measurements of each beam particle and expressed in equation 3. The distribution of D_x for a number of beam particles is shown in Fig.7.

$$D_x = \sum_{i=1}^4 a_i \cdot x_i \quad (3)$$

where a_i are the coefficients which depend on the distance of the chambers from the analyzing magnet and x_i are transverse position of the beam particle measured in the drift chambers. We adjusted the maximum drift time so that the width of the D_x distribution is the narrowest. The quantity of the maximum drift time gives us the drift velocity.

The width of D_x distribution is related to the resolution of the chamber stations, σ_x , and Coulomb multiple scattering effects by

$$\sigma_{D_x}^2 = \sigma_x^2 \sum_{i=1}^4 a_i^2 + \sigma_{\theta_{Coulomb}}^2 \cdot Z_{eff}^2 \quad (4)$$

$$\sigma_{\theta_{Coulomb}}^2 \cdot Z_{eff}^2 = \left(\frac{E_0}{E}\right)^2 (t_2 \cdot z_2^2 + t_3 \cdot z_3^2) = \left(\frac{E_0}{E}\right)^2 \cdot t \cdot \frac{t_2 \cdot z_2^2 + t_3 \cdot z_3^2}{t_2 + t_3}, \quad (5)$$

where t_2 and t_3 are the relative material thickness around the drift chambers

DC2 and DC3 in radiation length units (x_i/X_0), t is the full thickness, $t = t_2 + t_3$, z_i is the distance from the drift chamber to the center of the magnet, E is an electron energy, E_0 is equal to 13.6 MeV. Z_{eff} is the effective distance from the center of the magnet to the scattering center given by

$$\frac{t_2 \cdot z_2^2 + t_3 \cdot z_3^2}{t_2 + t_3} = Z_{eff}^2 \approx \frac{z_2^2 + z_3^2}{2} \approx (3.3 \text{ m})^2, \quad (6)$$

since $t_2 \approx t_3$. The equation (4) can be rewritten in the following way

$$\sigma_{D_x}^2 = S + \frac{C}{E^2}, \quad (7)$$

emphasizing the difference in the beam energy dependence of the two terms. We see that $\sigma_{D_x}^2$ is a linear function of $1/E^2$. We have the measurements of $\sigma_{D_x}^2$ for a set of energies. Fitting these data by a straight line we have found that

$$\sigma_{D_x}^2 = 0.219 + \frac{14.22}{E^2}$$

Therefore the position resolution of the DC station assuming that all the

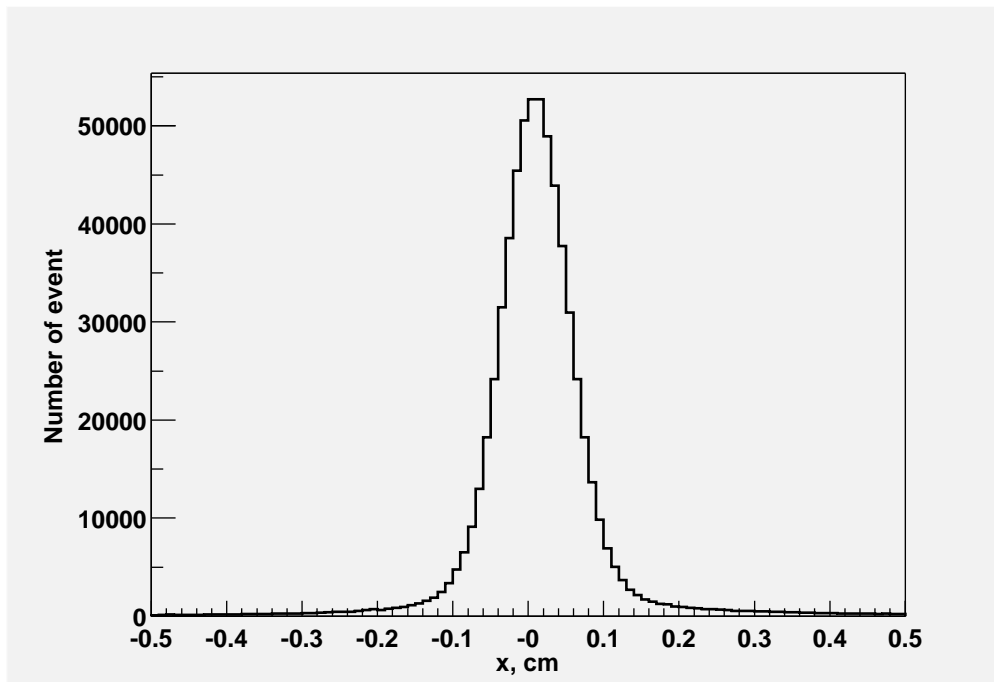


Fig. 7. Distribution of the lateral position difference in the center of the analyzing magnet for trajectories reconstructed by the upstream (DC1 and DC2) and downstream (DC3 and DC4) chambers.

Table 2

MC results and measured momentum detection precision. σ_p^* represents FWHM/2.35.

	Monte Carlo simulation		Measured values	
	No errors in DC	$\sigma_x=0.16$ mm	resolution	Beam momentum spread
Momentum, GeV/c	σ_p/p , %	σ_p/p , %	σ_p/p , %	σ_p^*/p , %
1.0	2.38±0.04	2.38±0.04	2.05	4.3
2.0	1.14±0.04	1.14±0.04	1.03	5.5
5.0	0.52±0.01	0.53±0.01	0.43	5.6
10.0	0.25±0.01	0.28±0.01	0.24	3.8
26.7	0.096±0.002	0.149±0.002	0.15	1.2
45.0	0.067±0.006	0.126±0.006	0.13	1.0

chambers have the same resolution is as follows:

$$\sigma_x^2 = \frac{S}{\sum_{i=1}^4 a_i^2} \quad (8)$$

$$\sigma_{\theta_{Coulomb}}^2 = \frac{C}{Z_{eff}^2} \cdot \frac{1}{E^2} \quad (9)$$

From (8) we found $\sigma_x = 0.16$ mm, which corresponds to a single chamber resolution to be $160 \cdot \sqrt{2}$. When we put (8) and (9) in equation (2), we obtain

$$\sigma_{\theta}^2 = \frac{S}{\sum_{i=1}^4 a_i^2} \cdot \sum_{i=1}^4 b_i^2 + \frac{C}{Z_{eff}^2} \cdot \frac{1}{E^2} \quad (10)$$

The results of the calculations using (10) are given in column 4 of the Table 2 as the measured values for a beam momentum resolution. The last column of the same table shows the measured by our spectrometer beam momentum spread (σ_p^*/p) in %, where σ_p^* represents FWHM/2.35 of the main peak since the momentum distribution is non-Gaussian.

The geometry of this beam line was reproduced in a GEANT Monte Carlo simulation taking into account the real materials distribution. The Moliere theory, corrected for finite angle scattering, was used to calculate the effect of multiple Coulomb scattering on the charged particle trajectory. The position resolution of each drift chamber station was taken as a Gaussian distribution with $\sigma_x = \sigma_y = 0.16$ mm. The momentum resolution was reconstructed using the same cuts as the real data. The results are presented in Table 2. Where,

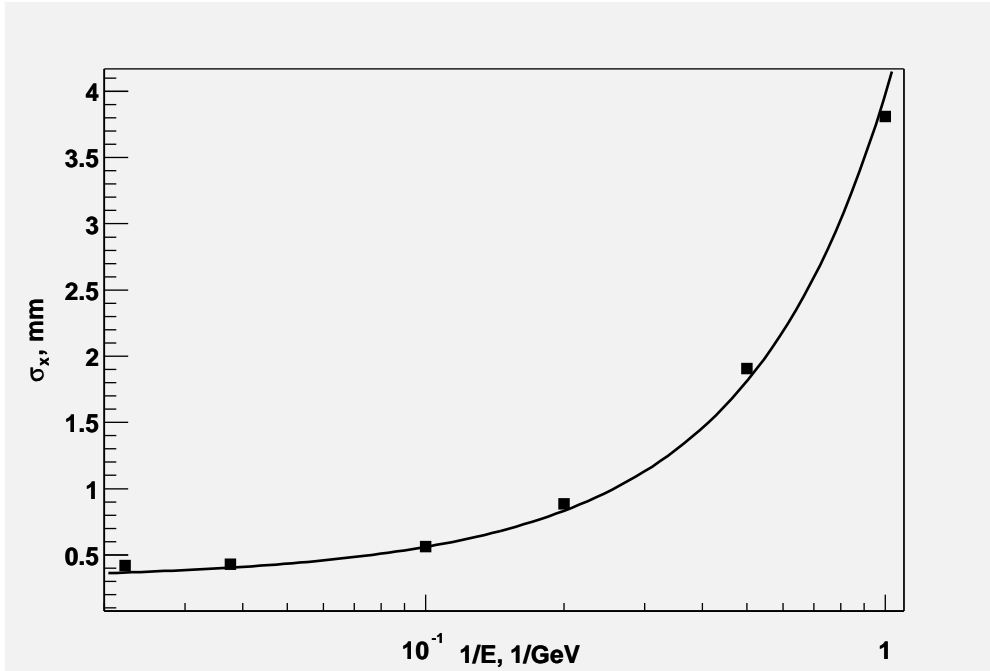


Fig. 8. Lateral distance distribution RMS dependence on energy. Solid line corresponds to MC-simulation results, filled squares real measurements.

σ_p/p is the relative error of the electron momentum. σ_x and σ_p are the r.m.s. of the Gaussian fit of the corresponding distribution.

The dependence of σ_{D_x} on energy was also simulated by GEANT. The results are shown in the Fig. 8. Solid line represents Monte Carlo simulation, filled squares real measurements. Estimated errors of the experimental data are inside the markers. There is a good agreement between the simulation data and the real measurements which are shown in Table 2 and Fig.8. It proves the validity of our drift chamber resolution determination described above.

6 Conclusion

The experience of long-term operation of a modified beam line for electrons with energies in the range of 1 to 45 GeV described in this paper shows that this technique significantly expands the possibilities to study precise energy and coordinate resolutions of scintillating crystals. Independent of the momentum spread of the electron beam at the level of 1 to 5% at energies from 45 down to 1 GeV, the momentum tagging station gives a beam momentum resolution from 0.13 to 2% in the same energy range. The precision is limited by drift chamber spatial resolution and multiple Coulomb scattering on a material in the beam line. GEANT Monte Carlo simulations of the resolution agree very well with the experimental results.

An opportunity to switch the beam line from electrons to high energy pions with high intensities (up to 10^6 e^- and 10^7 π^- per spill) allows the study radiation hardness properties of scintillating crystals both for electrons and hadrons with moderate dose rates of up to 100 rad/hour. These dose rates are similar to the ones that will be in BTeV at Fermilab and in CMS at CERN. Integrated doses up to several krad can be accumulated in this setup in a relatively short time.

7 Acknowledgments

We would like to thank the IHEP management for providing us a beam line and accelerator time for our testbeam studies. Special thanks to Fermilab for providing equipment for data acquisition. This work was partially supported by the U. S. National Science Foundation and the Department of Energy.

References

- [1] A.Kulyavtsev et al., Proposal for an Experiment to Measure Mixing, CP Violation and Rare Decays in Charm and Beauty Particle Decays at the Fermilab Collider - BTeV, May 2000.
- [2] A.I.Alikhanyan et al, Intern. Conf. Instr. for high energy physics, Dubna, 1970; Preprint IHEP 70-105, Serpukhov, 1970.
- [3] S.S.Gershrein et al, NIM, 112 (1973) 477-483.
- [4] A.M.Frolov et al, NIM, 216 (1983) 93-97.